Particle transport in ion and electron scale turbulence

A. Skyman[1], J. Anderson[1], L. Fazendeiro[1], H. Nordman[1], D. Tegnered[1], R. Singh[2] and P. Strand[1]

[1]Department of Earth and Space Sciences, Chalmers University of Technology
[2]Institute for Plasma Research, Gujarat, India

Corresponding Author: andreas.skyman@chalmers.se

Abstract:

Micro turbulent modes have important and non-trivial effects on transport in tokamaks. This paper deals with transport of main ions and impurities in ion and electron scale turbulence, driven by ion and electron temperature gradients, and trapped electrons. Using the gyrokinetic Vlasov code GENE, results are obtained from both nonlinear and quasi-linear simulations. The transport properties are quantified by calculating the gradient of zero particle flux for steady state in source free regions of the plasma. The results are compared and contrasted with results obtained using a computationally efficient fluid model. Of particular interest are conditions of steep gradients, relevant to e.g. transport barrier conditions. Further, results from a simple $\hat{s}$–α geometry are compared with results obtained using a JET-like magnetic equilibrium, and the effects on transport investigated.

1 Introduction

In the present work the turbulent transport of main ions and impurities in tokamaks driven by ion scale ion temperature gradient (ITG) and trapped TE (TE) modes, and electron scale electron temperature gradient (ETG) modes was studied. Nonlinear (NL) and quasi-linear (QL) gyrokinetic simulation results obtained with the code GENE [1][1] were compared with results from a computationally efficient fluid model [2]. In particular, the transport of particles in regions of steep density gradients, relevant to the pedestal region of H-mode plasmas, has been investigated.

The main focus of the work has been to obtain steady state particle profiles locally, determined from the balance between diffusive and advective fluxes in source-free regions. The sign of the advective particle velocity (pinch) and the particle density peaking, measured by the density gradient (R/L_n) for zero particle flux, was calculated. For ITG/TE mode turbulence, scalings were obtained for the particle peaking with the driving density and temperature gradients and the impurity charge number. For ETG mode turbulence,

[1]See `http://gene.rzg.mpg.de/` for details on the GENE code

TABLE I: Parameters for gyrokinetic simulations; † denotes scan parameters

	ITG:	TE:	ITG/JET-like:	ETG:
T_i/T_e:	1.0	1.0	1.02	1.0
$\hat{s}$:	0.8	0.8	0.75	1.0
q:	1.4	1.4	2.20	3.0
$\epsilon = r/R$:	0.14	0.14	0.17	0.3
$k_\theta \rho_s$:†	0.2	0.2	0.2–0.6	6.4, 12.8
n_e, $n_i + Z\, n_Z$:	1.0	1.0	1.0	1.0
n_Z *(trace)*:	10^{-6}	10^{-6}	10^{-6}	-
Z:†	2, 28	2, 28	2–74	-
$R/L_{n_{i,e}}$:†	1.0–5.0	1.0–5.0	2.7	20.0–45.0
$R/L_{T_i}, R/L_{T_Z}$:†	7.0	3.0	5.6	$2\, R/L_{n_{i,e}}$
R/L_{T_e}:†	3.0	7.0	5.6	$1.5\, R/L_{n_{i,e}}$

the main ion density gradient corresponding to zero particle flux, relevant to the formation and sustaining of the steep edge pedestal, was estimated.

Results for the impurity and background density peaking were obtained for ITG, TE and ETG mode dominated turbulence for the parameters shown in Table I. The main results were obtained for a circular $\hat{s}$–α tokamak equilibrium in the low β ($\beta \sim 10^{-4}$) regime, neglecting effects of plasma rotation. Effects of using a realistic tokamak equilibrium on the impurity peaking factors were also investigated.

2 Zero flux gradients

The particle transport for species j is derived from

$$\Gamma_j = \langle \delta n_j \vec{v}_{\vec{E}\times\vec{B}} \rangle = -D_j \nabla n_j + n_j V_j \tag{1}$$

where Γ_j is the particle flux and n_j the density of the species, and $\langle \cdot \rangle$ means a spatial averaging [3, 4]. On the right hand side of Eq. (1), the transport has been divided into a diffusive and an advective part. For the domain studied ∇n_j and ∇T_j are constant ($-\nabla n_j/n_j = 1/L_{n_j}$ and $-\nabla T_j/T_j = 1/L_{T_j}$). The flux can therefore be written

$$\frac{R\Gamma_j}{n_j} = D_j \frac{R}{L_{n_j}} + RV_j, \tag{2}$$

with R the major radius of the tokamak.

In the core region of the tokamak, advection ("pinch") and diffusion balance to give zero flux in steady state. The *zero flux peaking factor* quantifies this

$$0 = D_j \frac{R}{L_{n_j}} + RV_j \Leftrightarrow -\frac{RV_j}{D_j}\bigg|_{\Gamma_j=0} = \frac{R}{L_{n_j 0}} \equiv PF_j. \tag{3}$$

Thus PF_j is interpreted as the *gradient of zero particle flux*. For trace impurities D_Z and V_Z are independent of ∇n_Z. Eq. (2) is then linear in R/L_{n_Z}, and PF_Z can be found by fitting a straight line to flux data. In general, however, D_j and V_j may depend on ∇n_j, and PF_j has to be found explicitly from the zero flux condition.

2.1 Transport models

The fluid and gyrokinetic models employed have been described in detail elsewhere, see [4] and references therein, only a brief summary is given here.

The NL and QL GENE simulations were performed in a flux tube geometry, in a low β ($\beta = 10^{-4}$) s–α equilibrium [1, 5–7] as well as a realistic JET-like magnetic equilibrium obtained using the TRACER code. Effects of finite β, plasma shaping, equilibrium $\vec{E} \times \vec{B}$ flow shear and collisions have been neglected. The effects of collisions are known to be important for the turbulent fluctuation and transport levels [8], however, their effects on the impurity peaking factor have been shown to be small [9]. For a typical NL simulation for main ions, fully kinetic electrons, and one trace species, a resolution of $n_x \times n_y \times n_z = 96 \times 96 \times 24$ grid points in real space and of $n_v \times n_\mu = 48 \times 12$ in velocity space was chosen. For QL GENE simulations the box size was set to $n_x \times n_y \times n_z = 13 \times 1 \times 24$ and $n_v \times n_\mu = 64 \times 12$ respectively. The impurities were included self-consistently as a third species in the simulations, with the trace impurity particle density $n_Z/n_e = 10^{-6}$ in order to ensure that they have a negligible effect on the turbulence.

For the fluid simulations, the Weiland multi-fluid model [2] was used to derive the main ion, impurity, and trapped electron density response from the corresponding fluid equations in the collisionless and electrostatic limit. The fluid simulations include first order finite larmor-radius (FLR) effects for the main ions, and parallel main ion/impurity dynamics. The free electrons are assumed to be Boltzmann distributed. The equations are closed by the assumption of quasi-neutrality.

An eigenvalue equation for TE, ITG and ETG modes is thus obtained in the presence of impurities. A strongly ballooning eigenfunction with $k_\parallel^2 = (3q^2R^2)^{-1}$ valid for magnetic shear $s \sim 1$ is used [10]. The eigenvalue equation is then reduced to a system of algebraic equations that is solved numerically.

3 Main results

3.1 Self-consistent treatment of main ion and impurity peaking

The peaking factors for background and impurity species were calculated self-consistently by first calculating the background peaking factor for zero particle flux ($PF_e = R/L_{n_e 0}$) assuming trace levels of impurities. The impurity peaking factor ($PF_Z = R/L_{nZ0}$) was then calculated using this value for the background density gradient.

Results for the simultaneous peaking of impurities and background ions show that, for the parameters studied, the background density peaking is higher than or of the same order as that of the impurities for both ITG and TE mode driven turbulence; see

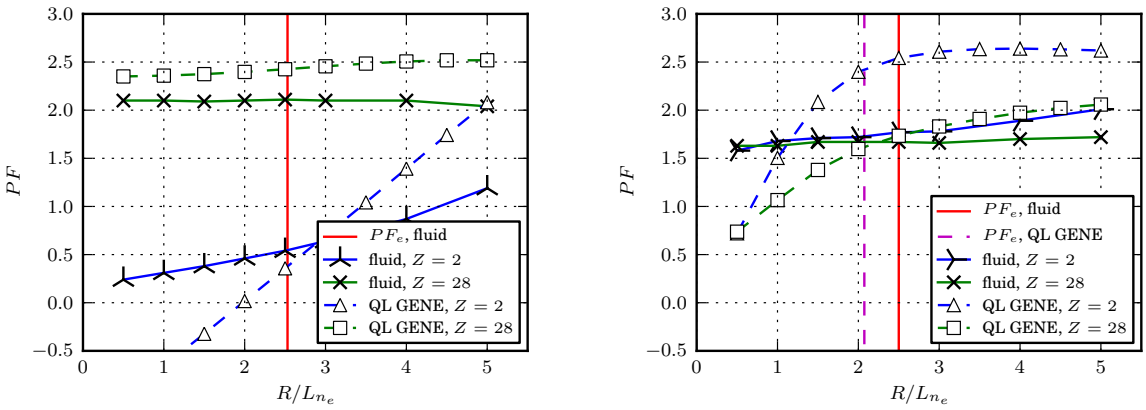

(a) dependence of the impurity density gradient of zero flux (PF) on the normalised electron density gradient for the ITG case, also indicated is the main ion peaking factor (PF_e) from fluid theory

(b) dependence of the impurity density gradient of zero flux (PF) on the normalised electron density gradient for the TE case, also indicated is the main ion peaking factor (PF_e) from fluid theory

FIG. 1: Scalings of the impurity density gradient of zero flux (PF) with the electron density gradient ($-R\nabla n_e/n_e = R/L_{n_e}$); also indicated is the main ion peaking factor (PF_e). Parameters as in Table I.

Fig. 1. The QL gyrokinetic and fluid model showed a good qualitative agreement, both significantly below neo-classical predictions for both impurity and main ion peaking [4].

3.2 Effects of realistic geometry on impurity transport

Simulations of impurity transport using a realistic *JET*-like magnetic equilibrium were compared to simulations with $\hat{s}$–α-geometry for an ITG dominated discharge. Parameters were chosen to correspond closely to *JET L-mode discharge #67730*, with parameters as in Table I and elongation $\kappa = 1.37$ at $r/a = 0.5$. The magnetic equilibrium was obtained using the TRACER code.

With the realistic geometry the growthrate spectrum is destabilised and shifted towards higher $k_\theta \rho_s$. This is due to a modification of curvature and FLR effects in non-circular geometry, mainly due to elongation, and is consistent with the fluid results in [11].

Weaker scalings of PF_Z with Z were consistently observed, and the level at which PF_Z saturates for high Z was reduced in the realistic case; see Fig. 2b. The lower levels can be attributed to a reduction of the curvature pinch due the changed geometry. A large increase in PF_Z was observed for the He impurity in the realistic case. This is due to a change in sign of the (outward) thermopinch for low Z in the realistic case.

When comparing QL and NL results, the former show a more dramatic scaling than latter and the QL results tend to over-estimate PF_Z for high Z, as can be seen in Fig. 2a. NL and QL impurity pinch qualitatively agree with the results in [4, 12].

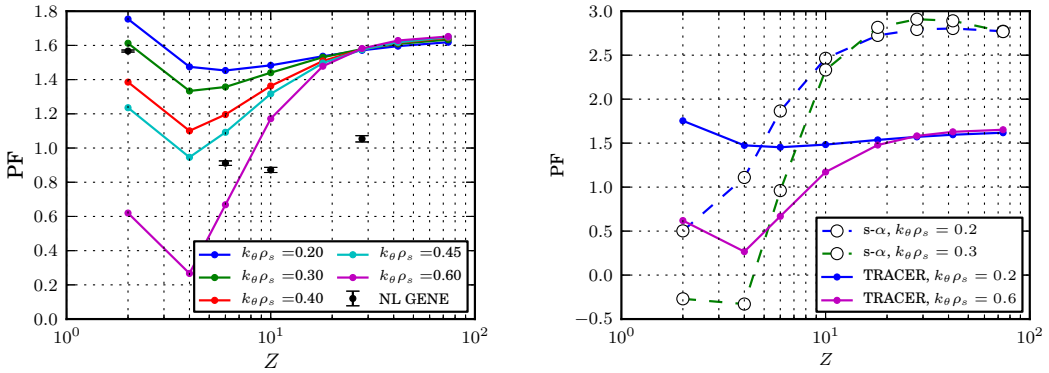

(a) comparison of QL and NL results

(b) comparison of $\hat{s}$–α and realistic magnetic geometry

FIG. 2: Scalings of impurity peaking factor (PF) with impurity charge (Z) for ITG dominated case with JET-like parameters; see Table I. The simple $\hat{s}$–α geometry was compared with a magnetic equilibrium obtained using the TRACER code.

3.3 ETG mode driven pinch under barrier like conditions

The ETG mode is driven by the electron temperature gradient and field curvature. It is analogous to the ITG mode, with the ion parameters replaced with their electron counterparts. The growthrate spectrum for the ETG mode has its maximum for $k_\theta\rho_e \approx 0.3$, with $\rho_e \approx \sqrt{m_i/m_e}\,\rho_s$. Using a reduced mass ratio of $m_i/m_e = 400$, this corresponds to $k_\theta\rho_s \approx 6.0$.

For ETG modes the focus is on the density gradient leading to zero main ion particle flux, related to the formation and sustaining of the edge pedestal. The parameters are chosen to correspond to barrier like parameters for *ASDEX Upgrade* [13], with

$$R/L_n = \frac{1}{2}R/L_{T_e} = \frac{2}{3}R/L_{T_i} \in [20.0,\, 45.0]; \tag{4}$$

see Table I for details on the parameters used.

Zero particle flux for the background was observed at very steep gradients for $k_\theta\rho_s$ consistent with ETG mode turbulence; see Fig. 3. As can be seen in figure Fig. 3b, $\omega_r < 0$ at the crossing points, which is consistent with electron modes.

For fluctuation level estimates for the ETG mode, see *TH/P7–04* by Anderson et al.

Acknowledgements

The simulations were performed on resources provided on the Lindgren[2] and HPC-FF[3] high performance computers, by the Swedish National Infrastructure for Computing

[2]See `http://www.pdc.kth.se/resources/computers/lindgren/` for details on Lindgren
[3]See `http://www2.fz-juelich.de/jsc/juropa/` for details on HPC-FF

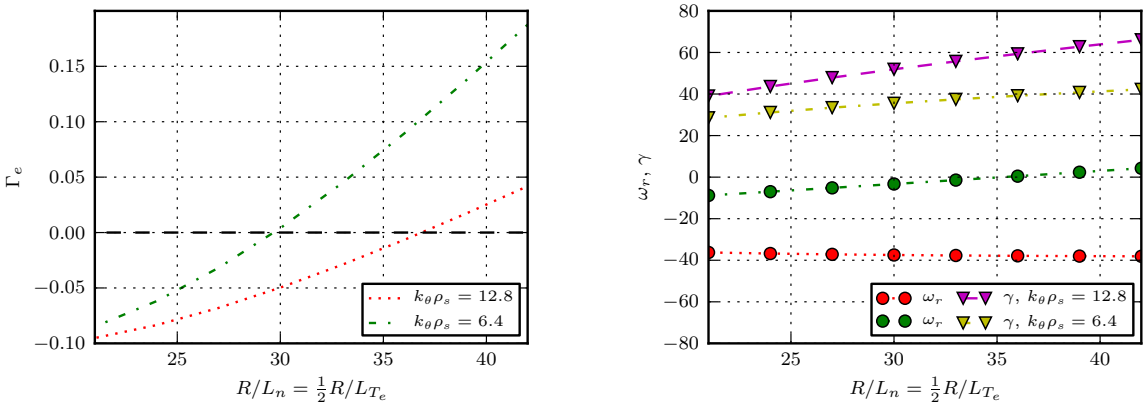

(a) electron particle flux *(b) growthrates (γ) and real frequencies (ω_r)*

FIG. 3: Scalings of electron particle flux and eigenvalues with the driving background gradients in the ETG mode driven, barrier like case. Parameters as in Table I.

(SNIC) at Paralleldatorcentrum (PDC) and the European Fusion Development Agreement (EFDA), respectively.

The authors would also like to thank F. Jenko, T. Görler, F. Merz, M.J. Püschel, D. Told, and the rest of the GENE team at IPP–Garching for their valuable support and input.

References

[1] F. Jenko, W. Dorland, M. Kotschenreuther, and B. N. Rogers. Electron temperature gradient driven turbulence. *Phys. Plasmas*, 7(5):1904, 2000.

[2] J. Weiland. *Collective Modes in Inhomogeneous Plasmas.* IoP Publishing, 2000.

[3] C. Angioni and A. G. Peeters. Direction of impurity pinch and auxiliary heating in tokamak plasmas. *Phys. Rev. Lett.*, 96:095003, 2006.

[4] H. Nordman, A. Skyman, P. Strand, C. Giroud, F. Jenko, F. Merz, V. Naulin, T. Tala, and the JET–EFDA contributors. Fluid and gyrokinetic simulations of impurity transport at JET. *Plasma Phys. Contr. F.*, 53(10):105005, 2011.

[5] T. Dannert. *Gyrokinetische Simulation von Plasmaturbulenz mit gefangenen Teilchen und elektromagnetischen Effekten.* Ph.d. thesis (monography), Technischen Universität München, 2005.

[6] T. Dannert and F. Jenko. Gyrokinetic simulation of collisionless trapped-electron mode turbulence. *Phys. Plasmas*, 12(7):072309, 2005.

[7] F. Merz. *Gyrokinetic Simulation of Multimode Plasma Turbulence.* Ph.d. thesis (monography), Westfälischen Wilhelms-Universität Münster, 2008.

[8] C. Angioni, J. Candy, E. Fable, M. Maslov, A. G. Peeters, R. E. Waltz, and H. Weisen.

Particle pinch and collisionality in gyrokinetic simulations of tokamak plasma turbulence. *Phys. Plasmas*, 16(6):060702, 2009.

[9] T. Fülöp, S. Braun, and I. Pusztai. Impurity transport driven by ion temperature gradient turbulence in tokamak plasmas. *Phys. Plasmas*, 17(6):062501, 2010.

[10] A. Hirose, L. Zhang, and E. Elia. Higher order collisionless ballooning mode in tokamaks. *Phys. Rev. Lett.*, 72(25):3993–3996, 1994.

[11] J. Anderson, H. Nordman, and J. Weiland. Effects of non-circular tokamak geometry on ion-temperature-gradient driven modes. *Plasma Phys. Contr. F.*, 42(5):545, 2000.

[12] A. Skyman, H. Nordman, and P. Strand. Impurity transport in temperature gradient driven turbulence. Submitted to Phys. Plasmas, 2011. URL `arXiv:1107.0880`.

[13] D. Told, F. Jenko, P. Xanthopoulos, L. D. Horton, E. Wolfrum, and ASDEX Upgrade team. Gyrokinetic microinstabilities in ASEDX Upgrade edge plasmas. *Phys. Plasmas*, 15(10):102306, 2008.